New Features in the Vortex Phase Diagram of $YBa_2Cu_3O_{7-\delta}$

K. Deligiannis,[1] P. A. J. de Groot,[1] M. Oussena,[1] S. Pinfold,[1] R. Langan,[1] R. Gagnon,[2] and L. Taillefer[2]
[1]*Physics Department, University of Southampton, Southampton SO17 IBJ, United Kingdom*
[2]*Physics Department, McGill University, Montreal, Quebec, Canada H3A 2T8*
(Received 1 May 1997)

Magnetic and transport measurements have been performed in high quality $YBa_2Cu_3O_{7-\delta}$ single crystals. We demonstrate for the first time that the magnetization peak line in the phase diagram of $YBa_2Cu_3O_{7-\delta}$, $H_p(T)$ exhibits an impressive similarity with the equivalent line for $Bi_2Sr_2CaCu_2O_8$. Our results show not only a similar temperature dependence but also an almost identical response to oxygen doping and a correlation to the multicritical point. At high temperatures we observe a previously unreported splitting of the magnetization peak. [S0031-9007(97)03985-9]

PACS numbers: 74.60.Ge, 74.72.Bk

Extended theoretical and experimental efforts to understand the vortex phase diagram in the high temperature superconducting oxides have led to as yet unexplained results. Contrary to serious arguments against the existence of a first order transition [1], in $Bi_2Sr_2CaCu_2O_8$ neutron diffraction and local Hall probe measurements [2] give evidence for such a transition line. In $YBa_2Cu_3O_{7-\delta}$, transport measurements give a first order transition evidence [3], while a specific heat verdict appears to be more conclusive [4]. At the same time, the vortex phases this first order transition separates are still under discussion. In $Bi_2Sr_2CaCu_2O_8$ the transition is more likely to be an evaporation of vortex liquid (decoupling) [5] or a sublimation of vortex solid [6], to uncorrelated pancakes. Coming to $YBa_2Cu_3O_{7-\delta}$, the candidacy of solid-to-liquid melting for the first order transition [3,4] is still unchallenged.

Another intriguing feature is the magnetic hysteresis anomaly observed in these oxides, namely, the increase of magnetization with magnetic field. In the past, proposed explanations have attributed the peak in magnetization to sample inhomogeneities, to a 3D to 2D vortex lattice transition, or to a crossover between bulk pinning and surface barriers [7]. In a recent study of the phase diagram in $Bi_2Sr_2CaCu_2O_8$ [8] it has been suggested that the peak effect there is produced by an unprecedented thermodynamic transition of the flux line lattice. In a less anisotropic material, like $YBa_2Cu_3O_{7-\delta}$, the reported peak in the magnetization, the "fishtail" peak, is so broad that it is unlikely to result from a relatively sharp thermodynamic vortex phase transition. In this Letter we map the peak position on the vortex phase diagram of $YBa_2Cu_3O_{7-\delta}$. We show for the first time that the resulting line can be directly related to the equivalent one in the phase diagram of $Bi_2Sr_2CaCu_2O_8$, exhibiting surprisingly similar temperature dependence and response to different oxygen doping. This universality is further strengthened when, combining transport and magnetic measurements, we find that the magnetization peak in $YBa_2Cu_3O_{7-\delta}$ correlates to the multicritical point.

The single crystals investigated were grown by a conventional self-flux method, using Y-stabilized zirconia crucibles, a method that gives crystals of very high purity ($\cong 99.9\%$). The high quality of the crystals investigated is further demonstrated by the observation of intrinsic pinning in magnetic measurements and current induced organization of vortex motion [9], both phenomena extremely sensitive to disorder. The details of the growth, oxygenation, and detwinning processes are described in Ref. [10]. We studied both twinned (TW) and detwinned (DT) crystals with various oxygen contents: 6.91 for crystals TW1, TW2, TW3, and DT2; crystal DT1 with oxygen contents of 6.90 (DT1A), 6.93 (DT1B), and 6.96 (DT1C); finally DT3 with 6.93 (DT3B) and 6.96 (DT3C) [11]. For the detwinned crystals, polarized light microscopy revealed a surface fraction of misaligned phase of less than 1%. The magnetic width of the superconducting transition of all crystals is $\Delta T_c < 0.3$ K. The oxygen concentration of the crystals has been assigned using data of Lagraff and Payne [12]. Thicknesses have been estimated using the mass and the theoretical density of 6.8 g/cm^3. Magnetic hysteresis measurements were carried out on a 12 T vibrating sample magnetometer and transport measurements were performed using a conventional four point ac method, with a resolution of 5 nV and in a field range of up to 14 T. Contacts to the samples were made by applying narrow pads of Ag epoxy on the crystal surface and curing for 1 h. In order to prevent change of oxygen content, the curing temperature was chosen equal to the annealing temperature.

Figure 1 reveals a new feature in the magnetic behavior of $YBa_2Cu_3O_{7-\delta}$ crystals. Data in this figure are from the same crystal but for two oxygen concentrations (DT1A and DT1B). Figure 1(a) shows magnetic hysteresis loops at various temperatures, from 60 to 78 K in steps of 2 K and for magnetic field ($\mathbf{H} \parallel c$) up to 12 T. These data are consistent with those reported in the literature by many groups [13]: The position of the main peak in magnetization goes to lower magnetic field values with increasing temperature. Figure 1(b) shows similar data for the same crystal but with a higher oxygen concentration. The hysteresis loops of Fig. 1(b) are taken from $T = 60$ K to $T = 72$ K in steps of 2 K.

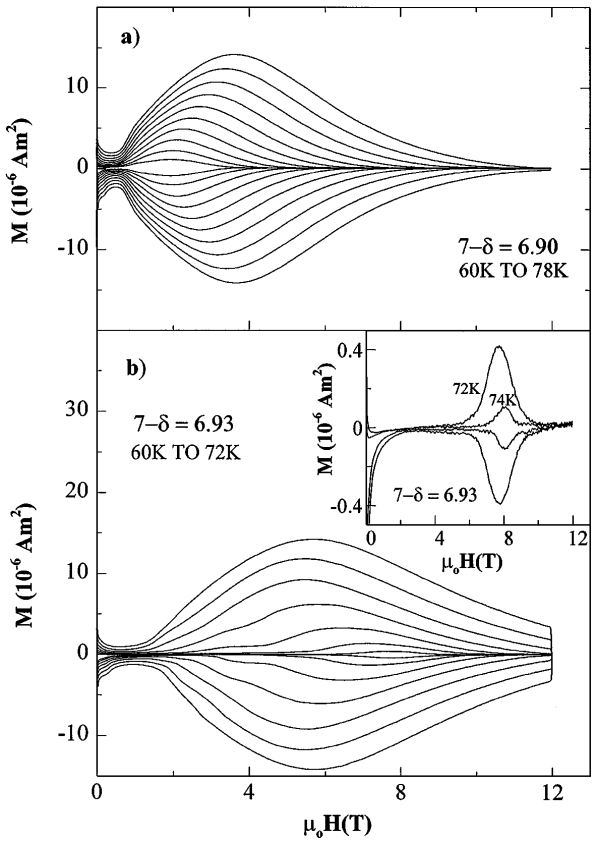

FIG. 1. Magnetic hysteresis loops of the same crystal but for two oxygen concentrations. Temperatures are as indicated; the outer *M-H* loop is taken at 60 K and for the inner ones, temperature is increased by steps of 2 K. Inset shows *M-H* loops close to the melting line.

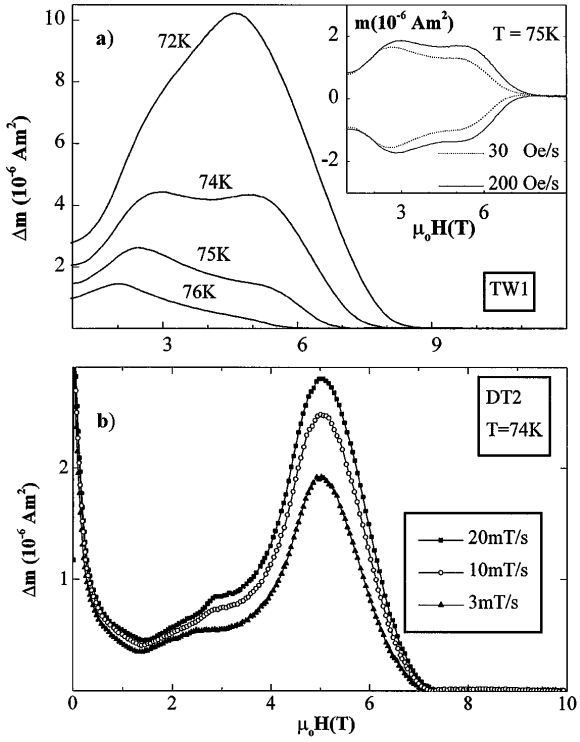

FIG. 2. (a) Hysteresis width vs applied field at 74 K and three magnetic sweep rates, for crystal DT2. (b) Hysteresis width vs applied field at the indicated temperatures. Inset shows *M-H* loop of crystal TW1, at 75 K and for two sweep rates.

The magnetization peak position occurs at higher field values as compared to Fig. 1(a). At $T = 60$ K the peak position changes by as much as 2 T; this large variation is a result of only a small change in the oxygen concentration. In addition, the main peak splits up into two peaks at high temperature. For this crystal the peak P_l, which occurs at low field, is observed only in a narrow temperature range. The second peak P_h, which occurs at higher magnetic field, narrows with increasing temperature and its position shifts to higher field values. The inset in Fig. 1(b) represents the peak P_h at $T = 72$ K and $T = 74$ K. The peaks are remarkably sharp for global magnetization measurements and the maximum hysteresis width is strongly temperature dependent: $\Delta M_{\max}(72\ \mathrm{K})/\Delta M_{\max}(74\ \mathrm{K}) \approx 4$. To the best of our knowledge, it is the first time that such features have been reported.

Figure 2(a) demonstrates how the fishtail magnetization peak builds up with decreasing temperature from 76 to 72 K in crystal TW1. Before going any further, we must stress that at high temperatures ($T > 65$ K) we have shown [14] that vortices are not localized to twin planes: There is no dependence of the magnetization on the angle between the applied magnetic field and the twin planes. Thus, twin planes do not localize vortices in the *V-I* window probed by magnetization measurements. Figure 2(a) clearly shows that the magnetic anomaly is a two step process. In this interesting crystal, we see how the two peaks P_l and P_h evolve with decreasing temperature before they merge to form the commonly named fishtail, at lower temperatures. Contrary to detwinned crystals, the peak P_l in microtwinned crystals survives and is observed in a broader temperature range; in some of them, up to 5 K below T_c. The inset depicts two hysteresis loops at $T = 75$ K and for two magnetic field sweep rates (and due to the field sweep rate and electric field equivalence, for two different voltage criteria): 3 and 20 mT/s. The peak P_l separates two different relaxation regimes. The maximum magnetic moment producing the peak P_h is observed to be strongly dependent not only on temperature as shown above, but also on the field sweep rate. Indeed, Fig. 2(b) exhibits at 74 K identical response of the two peaks, but for a detwinned crystal. In our measurements we have varied the sweep rate in the maximum available window, 3 to 20 mT/s, obtaining always the same result: The lower field peak P_l marks the onset of an increased relaxation rate and the position of the higher field peak P_h is voltage criteria independent.

Shown in Fig. 3 are the magnetization peak positions of microtwinned and detwinned crystals with the same

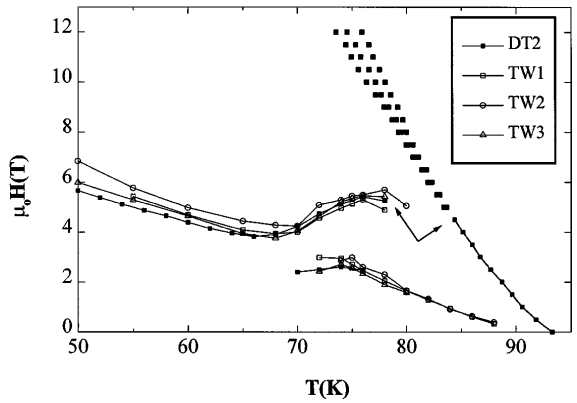

FIG. 3. Position, in the H-T plane, of the magnetization peak line for twinned and detwinned crystals of the same oxygen stoichiometry. Also represented are the melting lines, for crystal DT2, deduced from transport measurements with various voltage criteria. Arrows are a guide to the eye for magnetic data of DT2 and multicritical point.

oxygen concentration. In order to get the magnetic peak positions of microtwinned crystals at low temperatures ($T < 65$ K), hysteresis loops have been carried out with a magnetic field tilted away from twin planes by an angle of 10°. This angle is enough [14], in this temperature range, for vortices to break loose from twin planes and interact with them at points. At high temperature both peaks P_l and P_h are represented. Also shown in Fig. 3 is the melting line of crystal DT2, deduced from magnetotransport measurements with $\mathbf{H} \| c$ as described in Ref. [3]. A rapid drop of resistance observed at a well defined point (H_m, T_m) in the H-T plane for applied field $H < H_{\rm cp}$ was assigned [3] to a melting first order transition. For $H > H_{\rm cp}$, the resistive transition broadens and the melting line becomes voltage criteria dependent. The magnetic field $H_{\rm cp}$ plays the role of a multicritical point where the first order transition terminates, being replaced by a continuous, probably second order, solid-to-liquid transition [3,15]. For this crystal the broadening of the resistive transition takes place above $\mu_0 H_{\rm cp} = 4.5$ T. Following Fig. 3, we observe that this value is about the same as the magnetic field position of the peak P_h close to the melting line. This correlation of the peak field position to the multicritical point has not been previously reported. Measurements on twinned crystals, but with a magnetic field tilted away from twin planes by an angle of 7.5° (for the same reasons as above), lead to similar results.

Recently it was shown experimentally that the peak effect in $YBa_2Cu_3O_{7-\delta}$ is due to an elastic to plastic creep crossover [16], marking the nucleation of topological defects in the vortex system. Our results clarify even further the situation. We obtained a perfect fit for the position of peak P_l in the phase diagram, with the theoretical temperature dependence of the peak position resulting from the dislocations mediated plastic creep model [16]: $B_p(T) \propto [1 - (T/T_c)^4]^a$, with $a = 2$ [11]. However the fit is unsuccessful at lower temperatures, before the splitting of the fishtail peak. Indeed, Abulafia *et al.* [16] considered the model only in the temperature regime that P_l appears (around 80 K).

Thus, it becomes clear that the aforementioned model cannot account for the appearance of the peak at lower temperatures, before its splitting, and P_h. This resulting crossover line in the phase diagram, $H_p(T)$, exhibits on its own a surprising similarity with the equivalent, peak effect line for $Bi_2Sr_2CaCu_2O_8$. Lately, it was proposed [15,17] that $H_p(T)$ separates two distinct solid phases: a weakly disordered quasilattice associated with the Bragg glass phase [17] and a highly disordered entangled solid at higher fields [15]. These two phases, together with the liquid phase, connect to a multicritical point $(H_{\rm cp}, T_{\rm cp})$ [15]. In $Bi_2Sr_2CaCu_2O_8$, due to the sharpness of this vertical transition it was suggested that it represents a second order thermodynamic transition [8]. Coming back to our particular case, the additional observation of a voltage criteria *independent* peak, correlating to the multicritical point, seems to reinforce this scenario. In the comparison with $Bi_2Sr_2CaCu_2O_8$ one should also take into account the striking similarity in the temperature behavior of $H_p(T)$ in the phase diagram (Fig. 3). As in $Bi_2Sr_2CaCu_2O_8$ [8] the same nonmonotonic temperature dependence is observed. We went further and studied the response of $H_p(T)$ to different oxygen stoichiometry. Oxygen doping decreases the out-of-plane anisotropy γ, leading to more isotropic samples. In $Bi_2Sr_2CaCu_2O_8$ it was shown by Khaykovich *et al.* [8] that oxygen doping shifts $H_p(T)$ to higher fields in the phase diagram.

Figure 4 illustrates the magnetic peak positions, in the phase diagram, for different oxygen concentrations. Data are from (two) crystals DT1A, DT1B, DT1C, and DT2. Though it is difficult to obtain the exact values of the oxygen concentration for δ close to 0, the final oxygen concentration of the crystals, as is commonly accepted [10,18], depends systematically on the annealing

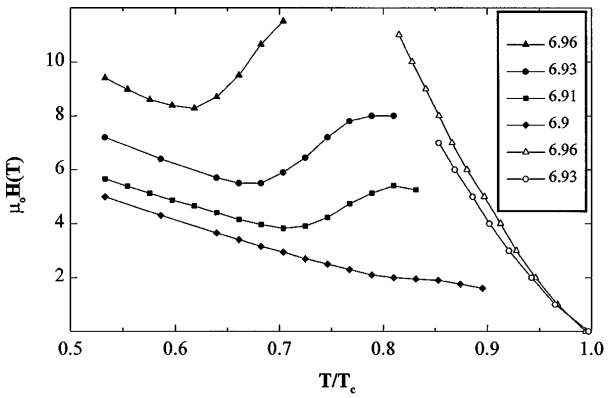

FIG. 4. Position, in the H-T plane, of the magnetization peak line, $H_p(T)$, and the melting line terminated at the multicritical point, for crystals with different oxygen concentrations.

temperature. Therefore, it increases undoubtedly as indicated in Fig. 4. As depicted, $H_p(T)$ shifts systematically and reversibly up and down in magnetic field, with the oxygen concentration increasing and decreasing, respectively. Similarly with $Bi_2Sr_2CaCu_2O_8$, the nonmonotonic temperature dependence of $H_p(T)$ strengthens with oxygen doping. Also in Fig. 4 is the melting line for two different oxygen concentrations of crystal DT3: DT3B and DT3C. At an oxygen content of 6.93 the multicritical point is found at 7 T, in agreement with $H_p(T)$. By doping the melting line is pushed upwards. We varied the field up to 11 T; however, no sign of broadening of the resistive drop at the first order transition was observed. This response provides impressive evidence for the universality of the phase diagram in the high-T_c superconducting oxides with weak random point disorder.

Theoretically, the field-driven transition of the vortex lattice is still not fully understood [15]. It involves disorder induced relative displacements of the order of α_0, the vortex lattice spacing, and finally permutation of neighboring vortices. The resulting configuration of twisted vortices can be characterized as an entangled solid [15]. Loss of translational and topological order of the vortex matter leads to the domination of dislocations. On the contrary, the existing Bragg glass phase below the transition retains translational order at long distances and perfect topological order [17]. Very recently it was pointed out that for the destruction of the Bragg glass not only the appearance of dislocations is important, but also the length scales that these dislocations appear relatively to α_0 [19]; in this frame, a scenario was proposed for $YBa_2Cu_3O_{7-\delta}$ which explains the peak effect at fields lower than the multicritical point. Our measurements strongly suggest that exactly as predicted by Giamarchi *et al.* [19], at high temperatures, thermally induced unbound dislocations invade the vortex system first at large length scales compared to α_0, affecting the critical current and producing a peak effect. However, the first order transition and the field-driven transition to the entangled state remain unaffected, since the relevant and important length scale for these transitions is α_0.

In conclusion, combining magnetic and transport data we demonstrated for the first time that the magnetization peak line $H_p(T)$ in the phase diagram of $YBa_2Cu_3O_{7-\delta}$ represents a well defined crossover which shifts to higher fields with oxygen doping and temperature, always correlating to the multicritical point. Our results show a surprising similarity with results for the highly anisotropic $Bi_2Sr_2CaCu_2O_8$, supporting the universality of the phase diagram for high-T_c superconducting oxides.

K. D. thanks G. Blatter, E. Zeldov, L. Krusin-Elbaum, T. Giamarchi, R. Doyle, and S. Gordeev for valuable comments. This work is part of a project supported by the EPSRC (U.K.). K. D. acknowledges the support of the Bodosaki Foundation (Greece) and L. T. the support of the Canadian Institute for Advanced Research and the Sloan Foundation.

[1] D. E. Farrell *et al.*, Phys. Rev. B **53**, 11 807 (1996); L. Radzihovsky, Phys. Rev. Lett. **74**, 4722 (1995).
[2] R. Cubbit *et al.*, Nature (London) **365**, 407 (1993); E. Zeldov *et al.*, Nature (London) **375**, 373 (1995).
[3] M. Charalambous *et al.*, Phys. Rev. B **45**, 5091 (1992); H. Safar *et al.*, Phys. Rev. Lett. **69**, 824 (1992); W. K. Kwok *et al.*, Phys. Rev. Lett. **69**, 3370 (1992).
[4] A. Schilling *et al.*, Nature (London) **382**, 791 (1996).
[5] R. A. Doyle *et al.*, Phys. Rev. Lett. **75**, 4520 (1995).
[6] B. Khaykovich *et al.* (to be published).
[7] M. Daeumling *et al.*, Nature (London) **346**, 332 (1990); G. Yang *et al.*, Phys. Rev. B **48**, 4054 (1993); N. Chikumoto *et al.*, Phys. Rev. Lett. **69**, 1260 (1992).
[8] B. Khaykovich *et al.*, Phys. Rev. Lett. **76**, 2555 (1996).
[9] M. Oussena *et al.*, Phys. Rev. Lett. **72**, 3606 (1994); S. N. Gordeev *et al.*, Nature (London) **385**, 324 (1997).
[10] R. Gagnon *et al.*, Phys. Rev. B **50**, 3458 (1994); R. Gagnon *et al.*, J. Cryst. Growth **121**, 559 (1993).
[11] K. Deligiannis *et al.* (to be published).
[12] J. R. Lagraff and D. A. Payne, Physica (Amsterdam) **212C**, 478 (1993).
[13] L. Krusin-Elbaum *et al.*, Phys. Rev. Lett. **69**, 2280 (1992); A. A. Zhukhov *et al.*, Phys. Rev. B **51**, 12 704 (1995).
[14] M. Oussena *et al.*, Phys. Rev. Lett. **76**, 2559 (1996).
[15] D. Ertas *et al.*, Physica (Amsterdam) **272C**, 79 (1996); V. Vinokur *et al.* (to be published).
[16] Y. Abulafia *et al.*, Phys. Rev. Lett. **77**, 1596 (1996).
[17] T. Giarmarchi *et al.*, Phys. Rev. Lett. **72**, 1530 (1994); Phys. Rev. B **52**, 1242 (1995).
[18] J. G. Ossandon *et al.*, Phys. Rev. B **45**, 12 534 (1992); V. Hardy *et al.*, Physica (Amsterdam) **232C**, 347 (1994).
[19] T. Giamarchi *et al.*, Phys. Rev. B **55**, 6577 (1997).